

Contents lists available at ScienceDirect

# Journal of Energy Chemistry

journal homepage: www.elsevier.com/locate/jechem



http://www.journals.elsevier.com/ iournal-of-energy-chemistry/

### Letter

## Highly converting syngas to lower olefins over a dual-bed catalyst

Zhaopeng Liu a,b,c,1, Youming Ni a,b,1, Xudong Fang a,b,c, Wenliang Zhu a,b,\*, Zhongmin Liu a,b,c,\*

- a National Engineering Laboratory for Methanol to Olefins, Dalian Institute of Chemical Physics, Chinese Academy of Sciences, Dalian 116023, Liaoning, China
- <sup>b</sup> Dalian National Laboratory for Clean Energy, Dalian Institute of Chemical Physics, Chinese Academy of Sciences, Dalian 116023, Liaoning, China
- <sup>c</sup> University of Chinese Academy of Sciences, Beijing 100049, China

#### ARTICLE INFO

Article history:
Received 10 September 2020
Revised 27 October 2020
Accepted 28 October 2020
Available online 6 November 2020

Keywords: Syngas Olefins Dual-bed SAPO-34 Dimethyl ether

© 2020 Science Press and Dalian Institute of Chemical Physics, Chinese Academy of Sciences. Published by ELSEVIER B.V. and Science Press. All rights reserved.

Light olefins ( $C_2$ – $C_4$  olefins) are the most important basic carbon-based building blocks, which are mainly produced from the catalytic cracking of naphtha [1–3]. With the rapid depletion of oil reserves and the growing demand for lower olefins, there is an urgent need to develop an alternative technique for producing them from non-petroleum resources such as coal, natural gas, or biomass. Currently, coal has been successfully transformed to olefins in China via the combination of the processes of coal-to-syngas, syngas-to-methanol and methanol-to-olefins [4–6]. In order to further improve efficiency and reduce investment, the direct conversion of syngas to olefins has received extensive attention in recent years [7].

There are three ways shown in Scheme 1 to convert syngas to olefins. Firstly, olefins can be produced by Fischer-Tropsch process (FTO) [8–10]. Because of the limitation of the Anderson-Schulz-Flory (ASF) distribution law [11–13], the selectivity of  $C_2$ – $C_4$  hydrocarbons is theoretically less than 58%. In recent years, owing to the precise design of the catalysts, the selectivity of olefins has reached nearly 60% for FTO process [10,14]. In 2016, Bao's group surprisingly obtained about 80% light olefins at 17% CO conversion over a physically mixed ZnCrAlO<sub>x</sub> and SAPO-34 catalyst [15]. This process was called as OX-ZEO STO. Almost simultaneously, Wang's team reported another mixed ZnZrO<sub>x</sub> and SAPO-34 catalyst, which

E-mail addresses: liuzhaopeng@tju.edu.cn (Z. Liu), wlzhu@dicp.ac.cn (W. Zhu), zml@dicp.ac.cn (Z. Liu).

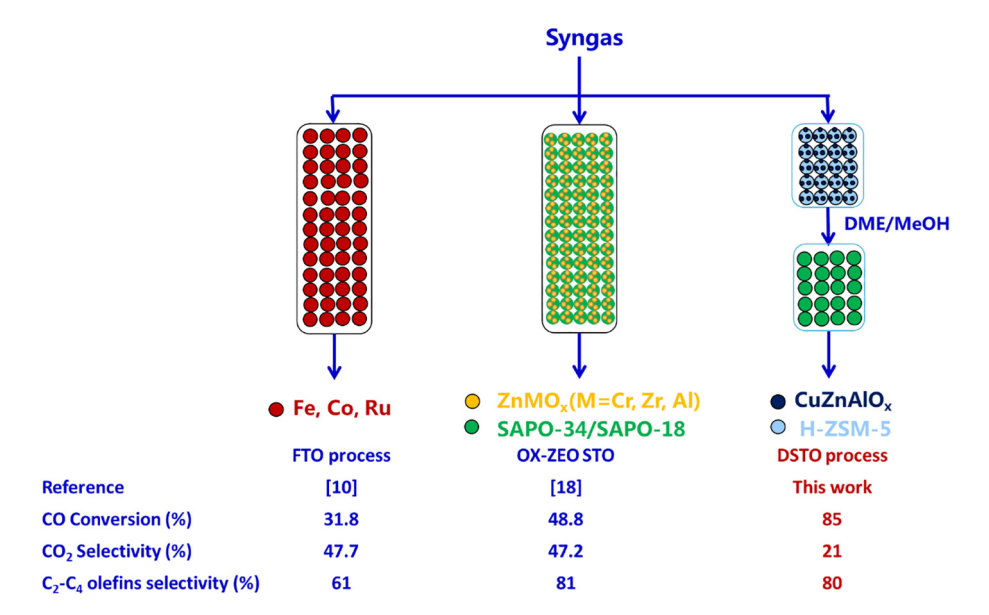
achieved the maximum selectivity of 74% light olefins at CO conversion of 9.2% [16]. Since then, the research on the synthesis of olefins from syngas based on mixed catalysts has received extensive attention and made great progress. Not long ago, Xie et al. reported over 80% light olefins at about 48% CO conversion over ZnCrO<sub>x</sub> and low-Si AlPO-18 mixed catalyst [17]. In 2019, the industrial pilot experiment of OX-ZEO STO process was successfully operated in Yulin, China. Besides FTO and OX-ZEO STO processes, our group has reported a dual-bed catalyst ZnAlO<sub>x</sub> (upper bed)/ SAPO-34 (lower bed), which reached 77.0% light olefins with only 33.1% CO<sub>2</sub> selectivity, which was called DSTO process [18]. The DSTO process proves that conversion of syngas to olefins can be achieved through syngas-to-dimethyl ether (STD) and dimethyl ether-to-olefins (DTO) in tandem. The dual-bed catalyst has many advantages in optimizing reaction conditions, withdrawing reaction heat, and regenerating the molecular sieve catalysts [19]. No matter which way is studied, high CO conversion with high lower olefins selectivity has always been the primary goal for syngas conversion to olefins.

Herein, we report 85% CO conversion and 80%  $C_2$ – $C_4$  olefins in hydrocarbon products with only 21%  $CO_2$  selectivity in syngas conversion over a dual-bed catalyst (CuZnAlO<sub>x</sub> + H-ZSM-5)/SAPO-34, which contains CuZnAlO<sub>x</sub> + H-ZSM-5 STD catalyst in upper bed and SAPO-34 DTO catalyst in the lower bed.

The dual-bed catalyst used in this work was composed by the physically mixed catalyst  $CuZnAlO_x + H-ZSM-5$  in upper bed and SAPO-34 molecular sieve in lower bed. A mixed catalyst named  $CuZnAlO_x + H-ZSM-5$  was made by mixing of granules  $(0.4^{\sim}$ 

<sup>\*</sup> Corresponding authors.

<sup>&</sup>lt;sup>1</sup> These authors contributed equally to this work.



**Scheme 1.** Three routes for converting syngas to olefins.

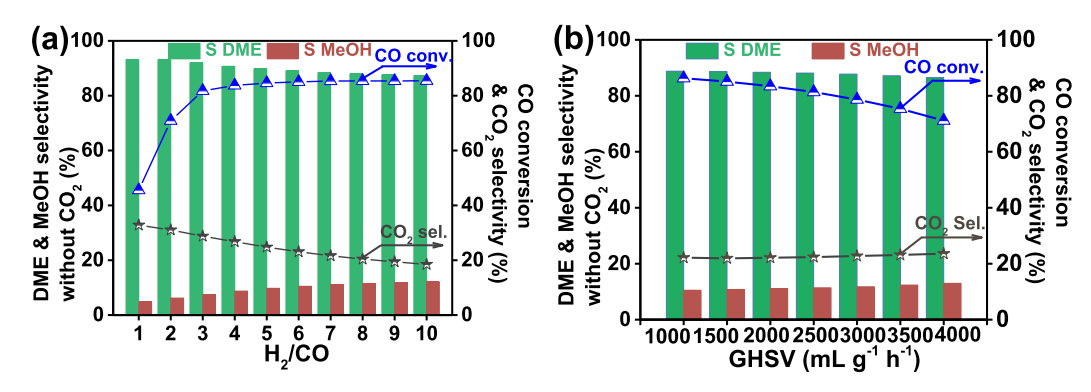


Fig. 1. STD results over  $CuZnAlO_x + H-ZSM-5$  catalyst. (a) The effect of  $H_2/CO$  molar ratio. Catalyst mass = 0.6 g; reaction temperature = 533 K; reaction pressure = 2.0 MPa; space velocity = 1500 mL  $g^{-1}$   $h^{-1}$ . (b) The effect of space velocity. Catalyst mass = 0.6 g; reaction temperature = 533 K, reaction pressure = 2.0 MPa;  $H_2/CO$  molar ratio = 7.

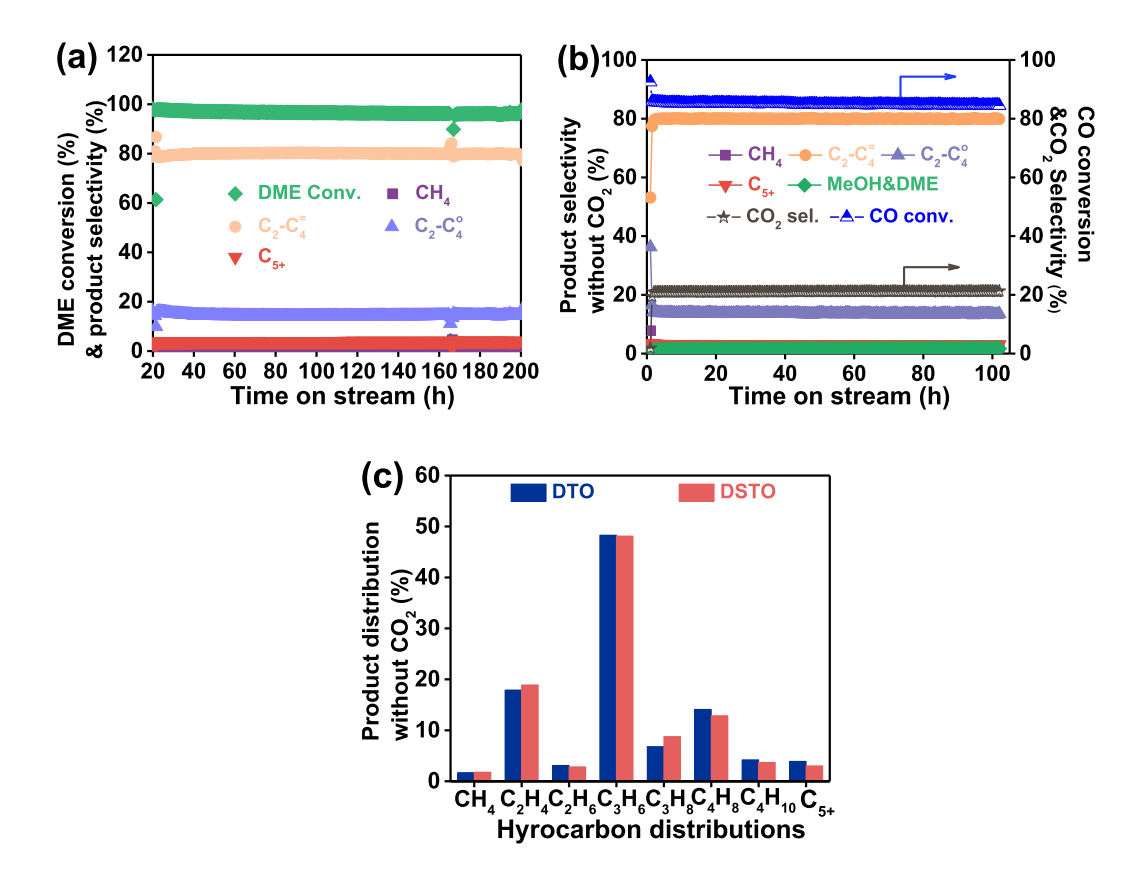
0.8 mm) of two components. The weight ratio of  $CuZnAlO_x/H-ZSM-5$  was 2/1. The  $CuZnAlO_x + H-ZSM-5$  loaded in the upper bed was utilized for STD reaction, meanwhile the SAPO-34 molecular sieve placed in the lower bed was used for DTO reaction. The weight ratio of upper bed catalyst/lower bed catalyst was 9/1.

SAPO-34 molecular sieve (XRD patterns shown in Fig. S6) and H-ZSM-5 zeolite (XRD patterns shown in Fig. S8) were identical to those in our previous work [18].  $CuZnAlO_x$  oxide (XRD patterns shown in Fig. S5) was commercial methanol synthesis catalyst. The ratio of silica to alumina in H-ZSM-5 was about 100, while the silica content in SAPO-34 was about 7%. The molar ratio of Cu:Zn:Al for  $CuZnAlO_x$  catalyst was 6:3:1.

Catalytic reaction experiments were performed in two fixed-bed stainless steel reactors (9 mm inner diameter) in tandem. Each bed was equipped with a temperature controller. The catalysts in dual-bed system were activated in  $H_2$  at 573 K (upper bed) and 723 K (lower bed) for 4 h. The syngas was introduced into the reaction system followed by activation. All products were kept in gas phase and analyzed online by an Agilent 7890B GC equipped with a HP-PLOT/Q capillary column connected to FID detector and a TDX-1 column connected to TCD detector.  $CH_4$  was used as a reference bridge between TCD and FID. Hydrocarbon selectivity was based on carbon atoms number. Hydrocarbons  $(C_nH_m)$ , MeOH and DME selectivity calculation methods (excluding  $CO_2$ ) were the same as our previous work [18].

In our previous work, we reported a dual-bed catalyst at 673 K, 4 MPa, which exhibited high  $C_2$ – $C_4$  olefins (~77%) and lower  $CO_2$  selectivity (~30%) [18]. The syngas to olefins reaction can be understood as the combination of STD and MTO reactions regardless of catalytic behaviors and mechanisms. However, in order to pursue a high CO conversion, the ZnAlO<sub>x</sub> spinel oxide as a STD catalyst and the high reaction temperature of 673 K are not the best choice. On the one hand, the higher the reaction temperature, the lower the thermodynamic equilibrium conversion is. In other words, for STD reaction, 673 K is too high. On the other hand, the performance of STD catalyst composed of conventional methanol synthesis catalyst CuZnAlO<sub>x</sub> and solid acid catalyst such as H-ZSM-5 may be much higher than ZnAlO<sub>x</sub>. Therefore, we select CuZnAlO<sub>x</sub> + H-ZSM-5 as upper STD catalyst for DSTO reaction.

First, we investigated the effect of the  $H_2/CO$  ratio on the STD behaviors over the  $CuZnAlO_x$  + H-ZSM-5 at 533 K, 2.0 MPa, 1500 mL  $g^{-1}$  h<sup>-1</sup>. As exhibited in Fig. 1(a), with increasing the  $H_2/CO$  ratio from 1:1 to 4:1, CO conversion is significantly increased from 45% to 85%, whereas the selectivity of DME is slightly decreased from 95% to 89%. It suggests that a higher  $H_2/CO$  ratio favors the conversion of CO, but does not benefit the selectivity of DME. After further increasing  $H_2/CO$  ratio, the DME selectivity and CO conversion are both slightly changed, which indicates that these values approach those predicted by the thermodynamic equilibrium model at the studied reaction conditions (Fig. S2)



especially at a  $\rm H_2/CO$  ratio > 7. Fig. 1(b) shows that CO conversions decrease almost linearly with space velocity, meanwhile the selectivity of DME, MeOH and  $\rm CO_2$  are slightly changed with space velocity rising.

We simulated the composition of outlet products for the STD process to explore the DTO process. Fig. 2(a) presents the DTO behavior over SAPO-34 under reaction conditions of 683 K, 2.0 MPa, space velocity = 15000 mL g<sup>-1</sup> h<sup>-1</sup> and  $H_2/CO/DME/CO_2/$ Ar = 75/10/5/5/5. It is surprising that the  $C_2-C_4$  olefins selectivity is as high as 81.5% at more than 98.1% DME conversion. In the meantime, the DTO reaction over SAPO-34 delivers a good stability in a 200 h test. As previous studies have proved that Brønsted acid of the SAPO-34 molecular sieve could catalyze olefins hydrogenation to paraffins [20,21], which would be the major challenge to DTO reaction. Thus, we investigated the effect of reaction conditions on DTO performance. As shown in Fig. S3(a), DME conversion is slightly increased with decreasing the space velocity from 15,000 to 5000 mL  $g^{-1}$   $h^{-1}$ , but the selectivity of  $C_2-C_4$  olefins is remarkably decreased with the space velocity decreasing. As increased reaction pressure from 2 to 4 MPa in Fig. S3(b), DME conversion is slightly changed, whereas the selectivity of C2-C4 olefins is markedly decreased from 80 to 69% with C2-C4 paraffins increased simultaneously. As shown in Fig S3(c), increasing the H<sub>2</sub>/DME ratio is disadvantageous to  $C_2$ - $C_4$  selectivity.

Improving space velocity, decreasing reaction pressure (Fig. S3 (b)), and reducing  $H_2/DME$  ratio (Fig. S3(c)) can all increase the selectivity of olefins because they are beneficial to weaken the hydrogenation of olefins.

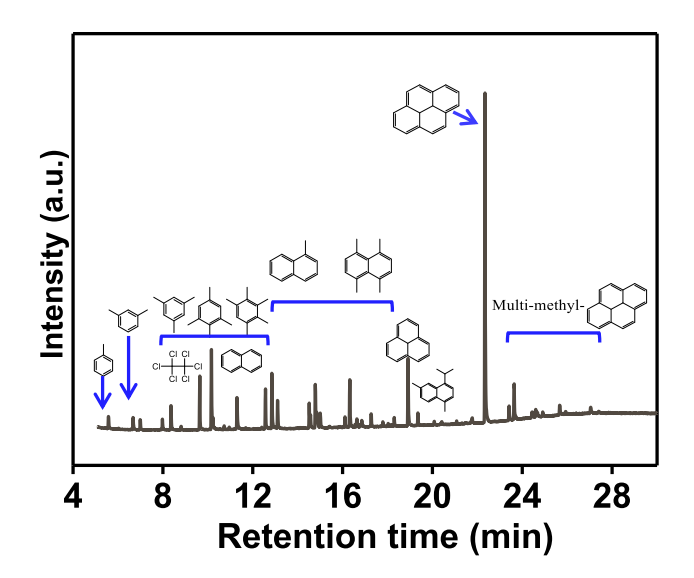


**Fig. 3.** GC–MS chromatograms of the organic materials retained in SAPO-34 components of spent dual-bed catalyst  $(CuZnAlO_x + H-ZSM-5)/SAPO-34$ .  $C_2Cl_6$  is used as the internal standard.

Syngas conversion over a dual-bed catalyst (CuZnAlO $_x$  + H-ZSM-5)/SAPO-34 was conducted at 533 K (upper bed), 683 K (lower bed), 2.0 MPa,  $\rm H_2/CO$  = 7/1 and space velocity = 1500 mL  $\rm g^{-1}$  h $^{-1}$ .

As shown in Fig. 3(b), the conversion of CO can reach as high as 85.1% with 80% C<sub>2</sub>–C<sub>4</sub> olefins selectivity (excluding CO<sub>2</sub>). The selectivity of C<sub>2</sub>-C<sub>4</sub> olefins in the previous reports can exceed 80% frequently, the CO conversion is generally low (Table S1) [10,16-18]. So far, the highest CO conversion in the OX-ZEO STO reaction could only reach about 48% [17]. It is apparent that compared to the OX-ZEO STO reaction, this DSTO reaction has a significant advantage in increasing the CO conversion and decreasing the CO<sub>2</sub> selectivity, which is beneficial to decrease the energy consumption for product separation and increase the atom economy. In our recent work [19], we proved that OX-ZEO STO could be considered as the combination of the STD and DTO reactions. The DTO reaction generally begins to start above 673 K, however, such high temperature is exactly unfavorable for CO conversion of the STD reaction (Fig. S1). This may be the essential cause of the low CO conversion in OX-ZEO STO reaction. It is worth mentioning that increasing the CO conversion is more valuable than increasing the H<sub>2</sub> conversion in reducing energy consumption of separating olefins, because H<sub>2</sub> has a small molecular weight and is easy to separate by some low-energy methods such as membrane. It can also be found in Fig. 3(b) that the selectivity of CO<sub>2</sub> is only about 21%, which is much lower than that (43%–50%) in OX-ZEO STO reaction. Lower CO<sub>2</sub> is beneficial to improve the utilization of CO. Moreover, the selectivity of CH<sub>4</sub> is less than 2%, and this dual-bed catalyst  $(CuZnAlO_x + H-ZSM-5)/SAPO-34$  is stable in 100 h on stream. Fig. S4(a) shows that CO conversions are close to that in the STD process (Fig. 1(b)) and decreased almost linearly with space velocity. The detailed product distributions excluding CO<sub>2</sub> produced by the WGS reaction are displayed in Fig. 2(c), which are consistent with that of DTO reaction catalyzed by SAPO-34 under the same pressure. Fig. S4(b) shows CO conversion and C2-C4 paraffins display a slight increasing trend with H<sub>2</sub>/CO ratio rising, while CO<sub>2</sub> selectivity presents a decreasing trend, which agrees with the results of the STD process.

To gain insights into the reaction paths over dual-bed catalyst  $(CuZnAlO_x + H-ZSM-5)/SAPO-34$ , soluble carbonaceous deposits in SAPO-34 after reaction were analyzed by GC–MS. Aromatic species such as methylbenzenes, methylnaphthalenes, phenanthrene, and pyrene can be observed in Fig. 3. These aromatic substances often act as hydrocarbon pool intermediates in the formation of olefins. Therefore, we believe that in the DSTO reaction, the formation of olefins still follows the conventional hydrocarbon pool mechanism, which is consistent with our previous conclusions [18].

As shown in Fig. S12, TG analysis indicates that less than 16% coke deposition (coke deposition rate of 0.56 mg g<sup>-1</sup> h<sup>-1</sup>) was eliminated after air treatment, which is lower than that reported in MTO process in high pressure hydrogen atmosphere. Lower carbon deposition rate could be attributed to the inhibition of hydrogenation transfer reaction and the occurrence of aromatics hydrogenation [22]. This may be the main reason for the long lifetime of the dual-bed catalyst (CuZnAlO<sub>x</sub> + H-ZSM-5)/SAPO-34 in DSTO process.

In conclusion, a dual-bed catalyst, which contains a syngas-to-DME mixed catalyst (CuZnAlO $_{\rm X}$  + H-ZSM-5) in the upper bed and a DME-to-olefins catalyst (SAPO-34) in the lower bed, can achieve 85% CO conversion, and 80% C $_{\rm 2}$ -C $_{\rm 4}$  olefins in hydrocarbon products with only 21% CO $_{\rm 2}$  selectivity in syngas conversion under 2.0 MPa. This dual-bed catalyst is very stable within 100 h on stream. The

reaction temperatures of two beds (including STD and DTO catalysts) are controlled separately, which helps to reach their optimal reaction temperatures and obtain better reaction performances. Because the dual-bed catalyst has many advantages in optimizing reaction conditions, withdrawing reaction heat, and regenerating the catalyst, it is promising in industrial applications.

#### **Declaration of Competing Interest**

The authors declare that they have no known competing financial interests or personal relationships that could have appeared to influence the work reported in this paper.

### Acknowledgments

We acknowledge the financial support from the National Natural Science Foundation of China (Grant Nos. 21978285, 21991093, 21991090), and the "Transformational Technologies for Clean Energy and Demonstration", Strategic Priority Research Program of the Chinese Academy of Sciences (Grant No. XDA21030100).

#### Appendix A. Supplementary data

Supplementary data to this article can be found online at https://doi.org/10.1016/j.jechem.2020.10.050.

#### References

- [1] A. Corma, F.V. Melo, L. Sauvanaud, F. Ortega, Catal. Today 107 (2005) 699–706.
- [2] G. Centi, E.A. Quadrelli, S. Perathoner, Energ Environ. Sci. 6 (2013) 1711–1731.
- [3] R. Diercks, J.D. Arndt, S. Freyer, R. Geier, O. Machhammer, J. Schwartze, M. Volland, Chem. Eng. Technol. 31 (2010) 631–637.
- [4] P. Tian, Y.X. Wei, M. Ye, Z.M. Liu, ACS Catal. 5 (2015) 1922–1938.
- [5] X.Q. Wu, S.T. Xu, W.N. Zhang, J.D. Huang, J.Z. Li, B.W. Yu, Y.X. Wei, Z.M. Liu, Angew. Chem. Int. Ed. 129 (2017) 9039–9043.
- [6] M. Yang, D. Fan, Y.X. Wei, P. Tian, Z.M. Liu, Adv. Mater. 31 (2019) 1902181– 1902195.
- [7] W. Zhou, K. Cheng, J.C. Kang, C. Zhou, V. Subramanian, Q.H. Zhang, Y. Wang, Chem. Soc. Rev. 48 (2019) 3193–3228.
- [8] H.M.T. Galvis, J.H. Bitter, C.B. Khare, M. Ruitenbeek, A.L. Dugulan, K.P. De Jong, Science 335 (2012) 835–838.
- [9] X.P. Zhou, J. Ji, D. Wang, X.Z. Duan, G. Qian, D. Chen, X.G. Zhou, Chem. Commun. 51 (2015) 8853–8856.
- [10] L.S. Zhong, F. Yu, Y.L. An, Y.H. Zhao, Y.H. Sun, Z.J. Li, T.J. Lin, Y.J. Lin, X.Z. Qi, Y.Y. Dai, Nature 538 (2016) 84–100.
- [11] H.M.T. Galvis, K.P. De Jong, ACS Catal. 3 (2013) 2130-2149.
- [12] R.A. Friedel, R.B. Anderson, J. Am. Chem. Soc. 72 (1950) 838–845.
- [13] R. Snel, Catal. Rev. Sci. Eng. 29 (1987) 361–445.
- [14] Y.Y. Dai, Y.H. Zhao, T.J. Lin, S.G. Li, F. Yu, Y.L. An, X.X. Wang, K. Xiao, F.F. Sun, Z. Jiang, Y.W. Lu, H. Wang, L.S. Zhong, Y.H. Sun, ACS Catal. 9 (2019) 798–809.
- [15] F. Jiao, J.J. Li, X.L. Pan, J.P. Xiao, H.B. Li, H. Ma, M.M. Wei, Y. Pan, Z.Y. Zhou, M.R. Li, S. Miao, J. Li, Y.F. Zhu, D. Xiao, T. He, J.H. Yang, F. Qi, X.H. Bao, Science 351 (2016) 1065–1068.
- [16] K. Cheng, B. Gu, X.L. Liu, J.C. Kang, Q.H. Zhang, Y. Wang, Angew. Chem. Int. Ed. 128 (2016) 4803–4806.
- [17] J.J. Su, H.B. Zhou, S. Liu, C.M. Wang, W.Q. Jiao, Y.D. Wang, C. Liu, Y.C. Ye, L. Zhang, Y. Zhao, H.X. Liu, D. Wang, W.M. Yang, Z.K. Xie, M. He, Nat. Commun. 10 (2019) 1297–1305.
- [18] Y.M. Ni, Y. Liu, Z.Y. Chen, M. Yang, H.C. Liu, Y.L. He, Y. Fu, W.L. Zhu, Z.M. Liu, ACS Catal. 9 (2018) 1026–1032.
- [19] Y.F. Hou, J.F. Li, M. Qing, C.L. Liu, W.S. Dong, Mol. Catal. 485 (2020) 110824–110832.
- [20] S. Senger, L. Radom, J. Am. Chem. Soc. 122 (2000) 2613-2620.
- [21] J. Kanai, J.A. Martens, P.A. Jacobs, J. Catal. 133 (1992) 527-543.
- [22] X.B. Zhao, J.Z. Li, P. Tian, L.Y. Wang, X.F. Li, S.F. Lin, X.W. Guo, Z.M. Liu, ACS Catal. 9 (2019) 3017–3025.